Proof of Concept of Acoustic Detection of Boiling Inception and State Transition Using Deep Neural Network

Yoshitaka Ueki[1,§], Kuniaki Ara[2]

[1] Department of Mechanical Engineering, Osaka University,
2-1 Yamadaoka, Suita, Osaka 565-0871, Japan
[2] Japan Atomic Energy Agency,
4002, Naritacho, Oarai, Ibaraki, 311-1393, Japan

[§]Correspondence author. Tel & Fax: +81-6-6879-4987
E-mail: ueki@mech.eng.osaka-u.ac.jp

Abstract

We develop a deep neural network model capable of detecting the boiling inception and state transitions from boiling acoustic measurements. We characterize acoustic spectrums of water boiling with different heating surface geometries, heat flux, and degree of subcooling. Our measurement result shows that the feature extraction of the boiling inception and state transition is possible from the boiling-sound frequency dataset in each specific target system. Notably, the deep neural network can distinguish the boiling inception and the state transition more accurately even at the high-level white-noise intensity where human beings and traditional data analysis methods cannot distinguish. This result suggests that the acoustic diagnosis with the deep neural network algorithm has great potential to detect the boiling inception and to monitor the boiling states in quasi-real-time during an early stage of the boiling phenomena, in the nuclear power plants.

1. Introduction

Phase change phenomena are efficient processes to transfer thermal energy and have been utilized in various industrial applications. Especially, boiling heat transfer is the thermal energy transfer process accompanied by the phase change to the vapor phase from the liquid phase adjacent to the heat transfer wall heated above the boiling point. Boiling is a fundamental phenomenon seen in the process of steam generation, such as boilers and steam generators. In addition, to take advantage of the high heat transfer efficiency, boiling has been employed in numerous industrial applications, such as cooling systems and heat exchangers (e.g. [1]).

On the other hand, boiling sometimes has negative influences during operating plants and thermal equipment. One example is the coolant boiling phenomena in sodium-cooled fast reactors [2]. In the fast reactors, sodium boiling is an important safety issue. In the case of the boiling inception, there will be vapor voids inside the reactor cores. The voids can give

significant reactivity insertion to the reactor core, which might lead to an increase in the reactor output power. Without detection and safety mitigation of it, the boiling could proceed further to the film boiling. As a consequence of the burnout, nuclear fuel pins will be overheated and severely damaged. Already, considerable safety margins and measures have been deployed in the fast reactors. However, further improvement in the safety measures has been highly required since the Fukushima Daiichi nuclear power plant accident.

For the detection of boiling, the acoustic diagnosis has been considered as the effective method [3]. Sounds travel through the coolant and solid structural components. Therefore, acoustic detectors are allowed to be located apart from the reactor cores, which is the possible acoustic emission source in case of boiling. Low invasiveness is one of the advantages that acoustic diagnosis has. In addition, the velocity of sound is quite fast. Because of this, the acoustic diagnosis is potentially able to capture fast phenomena. Based on them, in the present study, we focus on the acoustic diagnosis for boiling detection. During actual plant operations, various noises will be emitted from various machinery. For example, coolant flow in the piping will emit vortex-sound noises. Coolant pumps will emit some mechanical noises as well. Among these background noises, we are required to detect and identify the boiling sound traveling through the plant components. It is a great challenge for us since conventional acoustic analyses are yet not effective enough to overcome the high-level noises which bury target acoustic signals.

Recent rapid improvement in computer performance and computation algorithms allows us high-performance machine learning, such as super-resolution (e.g. [4]) and image denoising (e.g. [5]). Machine learning technologies have the potential to detect boiling sound among the surrounding noises. Previously, machine learning was employed and evaluated for acoustic boiling detection [3]. However, judging from the limitation of computation resources and an immature deep neural network algorithm, we speculate that the effectiveness of acoustic detection was limited. Recently, deep learning was utilized for the prediction of boiling crisis by using acoustic measurement [6] and infrared thermometry measurement [7]. With the recently advanced deep learning technologies, we aim to develop the acoustic detection of the boiling inception and state transition in a noisy environment. In the present study, we assess the feasibility of distinguishing the boiling sound from superposed white noises using the deep neural network (DNN).

2. Data Acquisition of Boiling Sound

2.1. Boiling on Hot-Wire

For machine learning, we characterize fundamental boiling acoustics using distilled water. The first system configuration we investigate is the saturated pool boiling on a hot wire. The wire is made of platinum, 300 μm in diameter and 40 mm in heating length. The wire is submerged in a distilled water pool. The distilled water is thermostatted to be at the saturated temperature using the additional heater. To mitigate natural convection induced by the additional heater, a flow suppression plate is installed below the heated wire. Figure 1 illustrates a schematic drawing of a sound recording of the saturated nucleate boiling on the heated wire at the saturated temperature. A microphone is located outside the water container and records boiling sound.

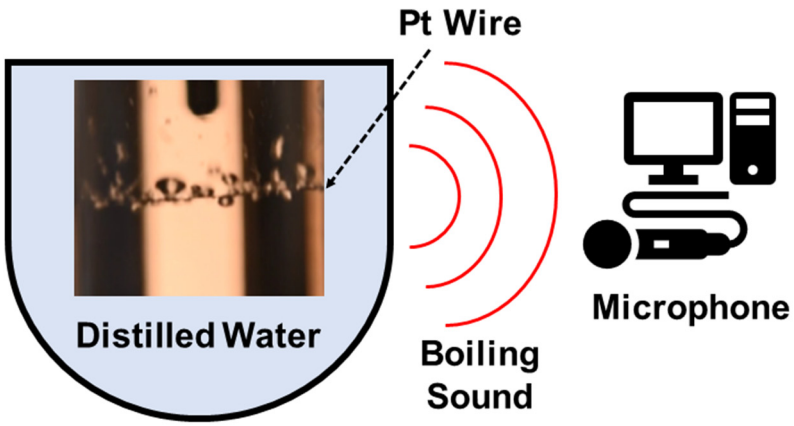

Figure 1. Schematic drawing of sound recording of saturated nucleate boiling on hot wire.

2.2. Boiling on Flat Heating Surface

Another test configuration is the pool boiling on a flat heating surface. Figure 2 illustrates a schematic drawing of a sound recording of the nucleate boiling on the flat heating surface. Distilled water is filled in a stainless container. The container bottom is heated by an electric heater. The boiling happens on the container bottom, that is the flat heating surface. A thermocouple is inserted into the distilled water to monitor the bulk water temperature. A hydrophone is mounted under the water to directly acquire the boiling sound. By using the hydrophone, we record the boiling sound at different liquid temperature T, which corresponds to the degree of subcooling, $\Delta T_{sub} = T - T_{sat}$.

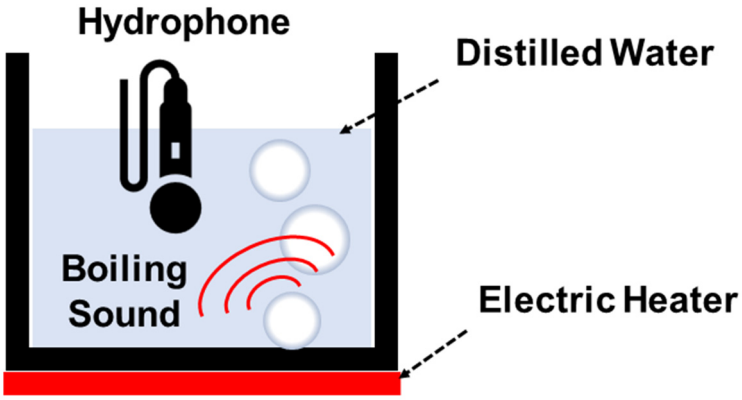

Figure 2. Schematic drawing of sound recording of nucleate boiling on flat heating surface.

3. Boiling Acoustics and Feature Extraction

3.1. Boiling on Hot-Wire

Figure 3 illustrates power spectrums of the saturated pool boiling on the hot-wire at different values of heat flux. The input data length for each power spectrums is 3 seconds. The heat flux of the hot-wire is evaluated from the following relation: $q = VI / \pi dl$. V denotes the voltage applied on the hot-wire. I denotes the electric current through the hot-wire. d and l denote the wire diameter and heating length. From Figure 3, notably, the characteristic frequency peak is located at approximately 500 Hz. As the heat flux increases, the characteristic frequency peak becomes more significant. This tendency is consistent with that reported in the previous study [8].

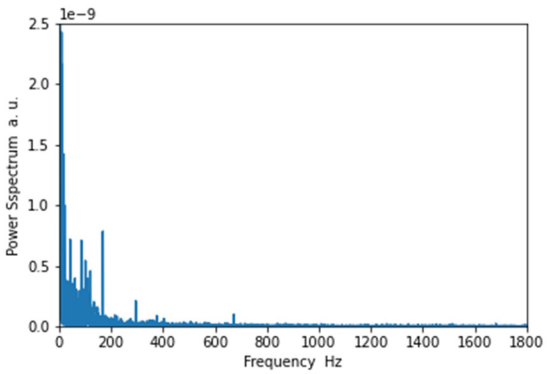

(a) Non-boiling regime.

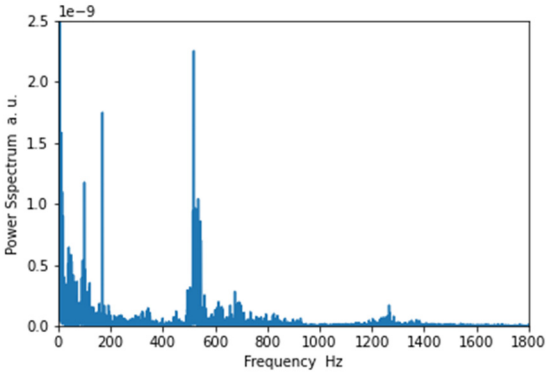

(b) Nucleate boiling (1.3×10^5 W/m^2).

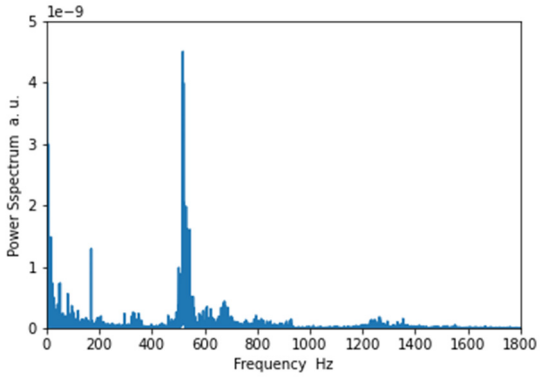

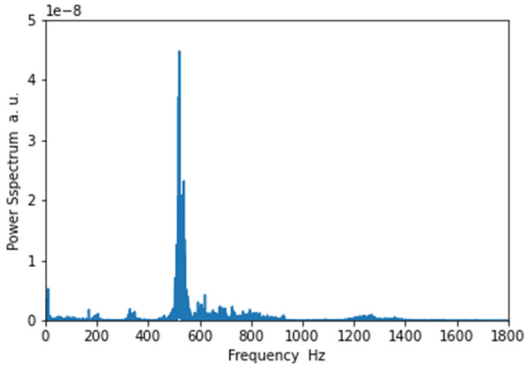

(c) Nucleate boiling (2.1×10^5 W/m^2). **(d) Nucleate boiling (4.8×10^5 W/m^2).**

Figure 3. Boiling sound frequency spectrums in the case of saturated pool boiling on hot-wire.

3.2. Boiling on Flat Heating Surface

Figure 4 illustrates power spectrums of the pool boiling on the flat heating surface at typical degrees of subcooling, which are approximately 25K, 15K, and saturated boiling. Besides a normalization, the method and procedures to calculate the power spectrums are identical as described above. From Figure 4 we find that the spectrum patterns, including the outstanding peak location, differ depending on the degree of the subcooling. In the case of the saturated boiling, the outstanding peak is located around 1100 Hz. It is different from the case of the boiling on the hot-wire. Different previous investigations on the acoustic detection in the saturated boiling region reported different frequency dominants [9-11]. However, the frequency dominants differed in the different investigations. We consider that influencing factors on the boiling sound emission are the boiling heat flux, the heating surface geometries, and the degree of subcooling. In the case of our hot-wire tests, the patterns of the boiling sound frequency spectrums are independent of the boiling heat flux. By considering them, we speculate that the boiling sound characteristics actually depend on the heating surface geometries. Even though, our measurement result shows that the feature extraction of the boiling inception and state transition is possible from the boiling-sound frequency dataset in each specific target system. The boiling sound frequency spectrums described above are employed as training data for the machine learning described below.

4. Test Data for Machine Learning

In the present study, we aim to evaluate the feasibility of distinguishing the above-mentioned boiling sound from the superposed white noises using the DNN. We generate and employ the test data by superposing the white noises which obey the Gaussian distribution with different values of standard deviation (SD) on the training data. Figure 5 illustrates the

generation of the test data from the training data. In the case of the higher value of the SD, the white noises become louder, and then the outstanding patterns of the boiling sound frequency spectrum become indistinguishable from the white noises.

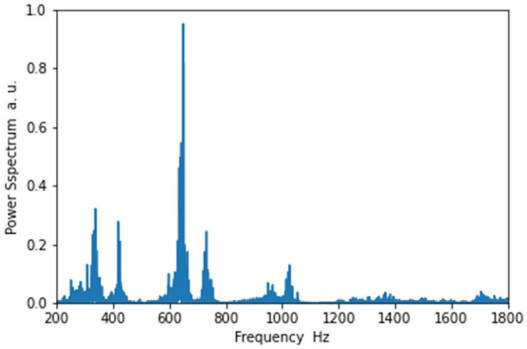

(a) Subcool boling ($\Delta T_{\text{sub}} \approx 25\text{K}$).

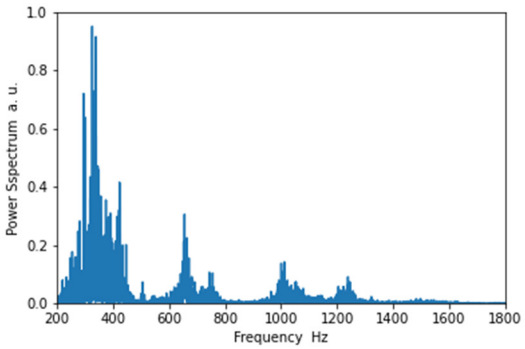

(b) Subcool boling ($\Delta T_{\text{sub}} \approx 15\text{K}$).

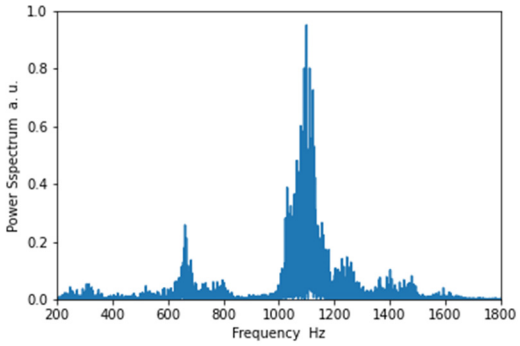

(c) Saturated boiling.

Figure 4. Boiling sound frequency spectrums in the case of pool boiling on flat heating surface at different subcooling.

5. Deep Learning of Boiling Acoustics

We employ the fully connected DNN architecture (see Figure 6). The input layer has 4800 units. The number of the hidden layers is 4. The first hidden layer has 2400 units, then reducing to 1200, 600, and 300 units through the rest of the hidden layers. The learning rate is 0.01. The activation functions are ReLU and Softmax. The softmax function is used just before the output layer. The optimizer is the stochastic gradient descent algorithm. The loss function is the sparse categorical cross-entropy. As for the classification of the hot-wire boiling, the output layer has 2 units, which corresponds to the states of the boiling and non-boiling. The epoch number is 20. As for the classification of the flat-surface boiling, the output layer has 3 units, which corresponds to 3 states of the degree of the subcooling. The epoch number is 250. We compare the multilayer perceptron (MLP), which has a single hidden layer, with the DNN algorithm to assess the DNN algorithm performance. The input and output layers have 4800 and 3 units, respectively. The hidden layer has 2400 units. The activation function is the

sigmoid function. Figure 7 shows the test results of detecting the boiling inception. At the relatively low white noise intensity, the accuracy of the DNN detection stays almost 100%. As the white noise becomes more intense, the accuracy decreases down to approximately 65% at the white noise intensity of 2 mV. From Figure 7 (b), as the white noise becomes more intense, the outstanding peaks of the boiling sound frequency are buried in the noise. It prevents the present DNN algorithm from accurate detection. Even though, notably, the DNN algorithm shows high performance at the high-level white-noise intensity. Figure 8 shows the test results of detecting the boiling state transition. At the relatively low white noise intensity, the accuracy of the DNN detection stays almost 100%. As the white noise becomes more intense, the accuracy decreases. The trend of the accuracy is similar to Figure 7. In the case of the MLP, the decrease in the accuracy drastically as the white noise becomes intense. It shows that the DNN algorithm is superior to the MLP even in the classification of the high-level noisy data.

6. Conclusions

Based on our analyses, we conclude that the feature extraction of the boiling inception and state transition is possible from the boiling-sound frequency dataset. The present study indicates that the boiling acoustics depend on the heating surface geometry. A further understanding of the boiling acoustics is necessary to develop the machine learning models generalized and more reliable. In conclusion, we have successfully performed the proof of concept that the DNN can distinguish the boiling inception and the state transition more accurately even at the high-level white-noise intensity where human beings and the traditional data analysis methods cannot distinguish. This result suggests that the acoustic diagnosis with the DNN algorithm has great potential to detect the boiling inception and to monitor the boiling states in quasi-real-time during an early stage of the boiling phenomena, in the nuclear power plants.

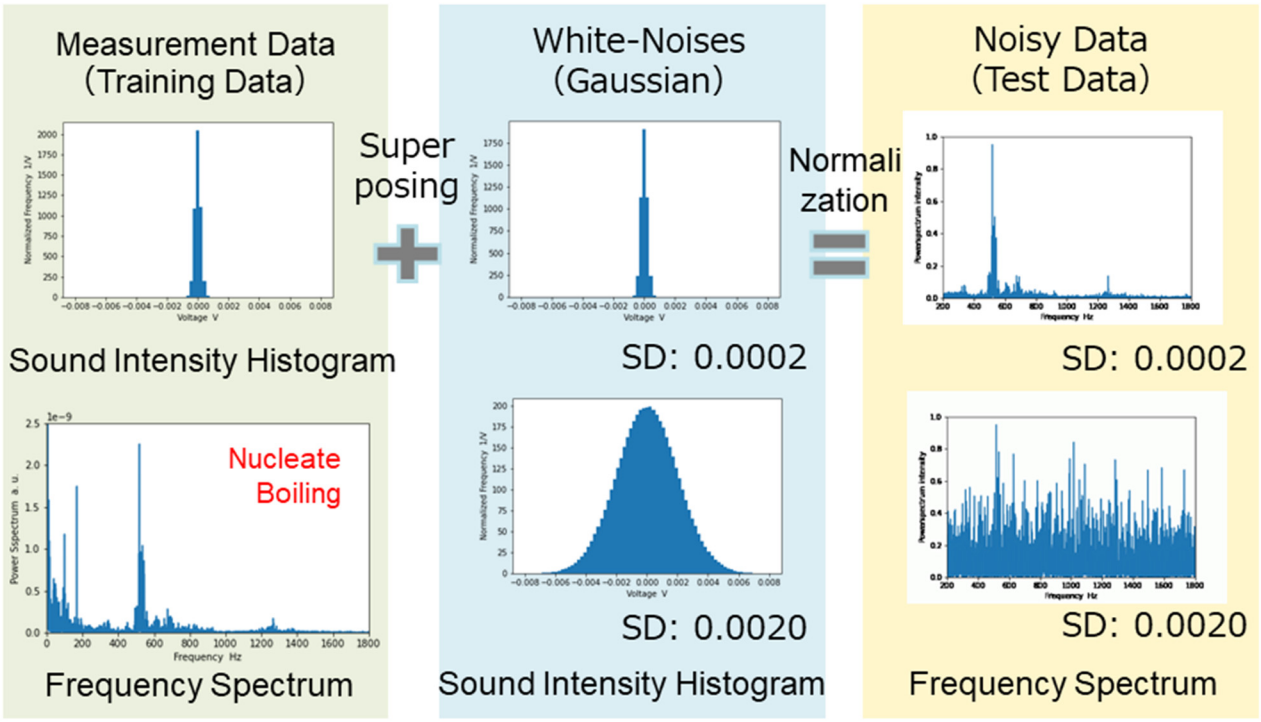

Figure 5. Generation of Test Data; Example of the case of saturated nucleate boiling on hot-wire.

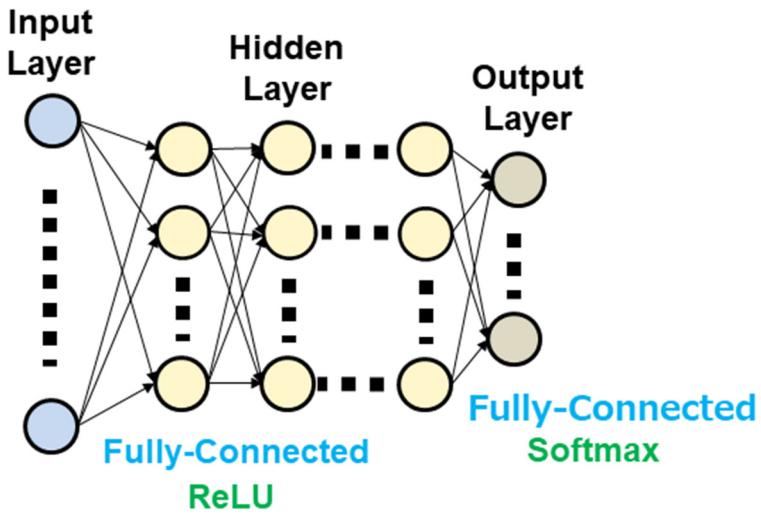

Figure 6. Schematic drawing of network architecture of DNN.

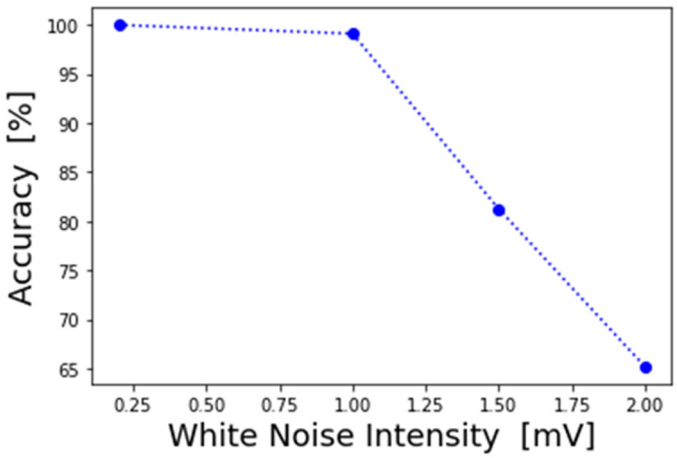

(a) Accuracy versus white noise intensity (SD).

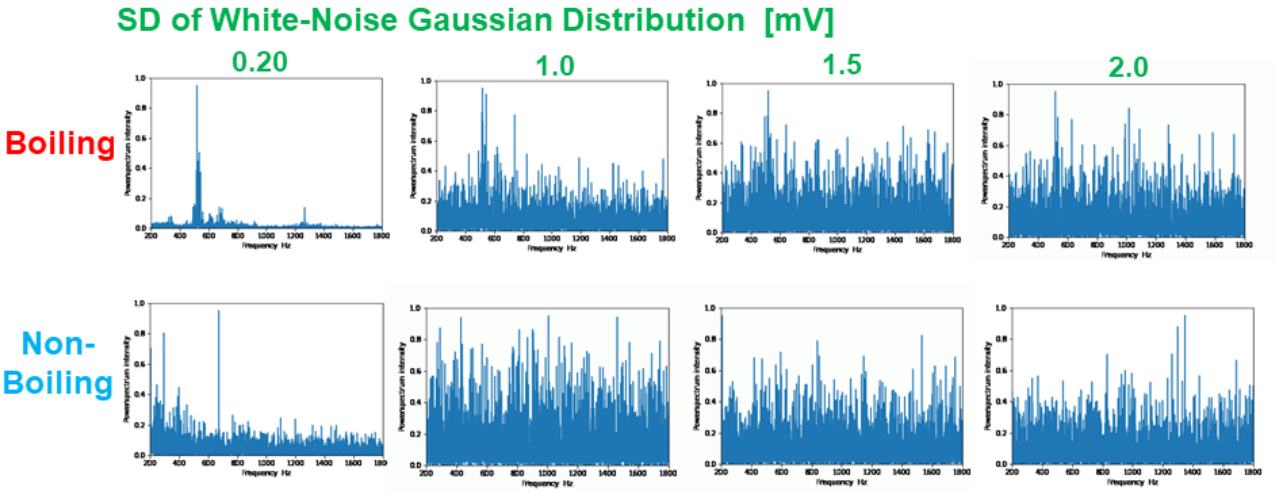

(b) Comparison of frequency spectrums at different intensities of white noises.

Figure 7. DNN performance in the case of boiling inception.

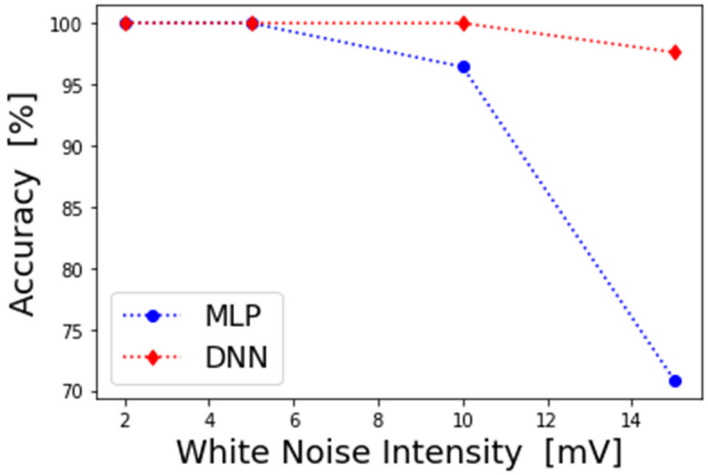

(a) Accuracy versus white noise intensity (SD).

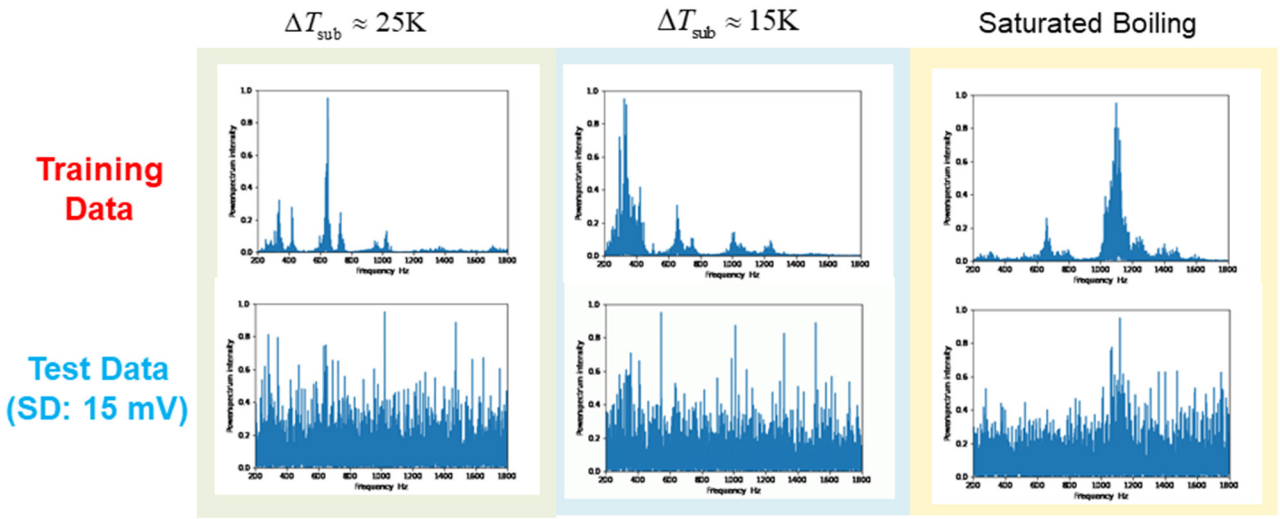

(b) Comparison of frequency spectrums at different intensities of white noises.

Figure 8. DNN performance in the case of boiling state transition.

Reference

[1] Yasuo Koizumi, Masahiro Shoji, Masanori Monde, Yasuyuki Takata, Niro Nagai, “Boiling: Research and Advances”, Elsevier (2017).

[2] Haileyesus Tsige-Tamirat, Sara Perez-Martin, Werner Pfrang, Marine Anderhuber, Antoine Gerschenfeld, Laurent Laborde, Konstantin Mikityuk, Christophe Peniguel, Stéphane Mimouni, “A Review of Models for the Sodium Boiling Phenomena in Sodium-Cooled Fast Reactor Subassemblies”, ASME Journal of Nuclear Engineering and Radiation, NERS-20-1117 (2021) https://doi.org/10.1115/1.4051066

[3] George Daniel Doney, “Acoustic Boling Detection”, Master Thesis, Massachusetts Institute of Technology (1994).

[4] Yu Chen et al., “FSRNet: End-to-End Learning Face Super-Resolution with Facial Priors”, arXiv:1711.10703 (2017).
[5] Jaakko Lehtinen et al., “Noise2Noise: Learning Image Restoration without Clean Data”, arXiv:1803.04189 (2018).
[6] Kumar Nishant Ranjan Sinha et al., “Deep learning the sound of boiling for advance prediction of boiling crisis”, Cell Reports Physical Science, **2**, 100382 (2021).
[7] Madhumitha Ravichandran et al., “Decrypting the boiling crisis through data-driven exploration of high-resolution infrared thermometry measurements”, Applied Physics Letters, **118**, 253903 (2021).
[8] M. Yuasa, “Microbubble emission boiling of heating wire at subcooling”, Master thesis of University of Tokyo (2004) (*in Japanse*).
[9] Akshat Negi, “Characterization of Boiling Sound at Conditions Approaching Critical Heat Flux”, Thesis. Rochester Institute of Technology (2019).
[10] F. L. Schwartz and L. G. Siler, “Correlation of Sound Generation and Heat Transfer in Boiling”, Journal of Heat Transfer, **87**(4), p. 436 (1965).
[11] S. B. Seo and I. C. Bang, “Acoustic analysis on the dynamic motion of vapor-liquid interface for the identification of boiling regime and critical heat flux”, International Journal of Heat and Mass Transfer, **131**, pp. 1138-1146 (2019).